Proceedings of the Korean Nuclear Society Spring Meeting

Cheju, Korea, May 2001

Numerical Analyses on a High-recycling Divertor Operation Regime in KSTAR Tokamak

Jin-Seok Ko and Sang Hee Hong
Seoul National University

Ki-Hak Im
Korea Basic Science Institute

Abstract

The operation space in a high-recycling divertor regime of the KSTAR tokamak is obtained in terms of the upstream density and the input power by numerical simulations with a two-dimensional two-fluid edge plasma transport code, EDGETRAN. The source terms for particles, momentum and energy in the edge transport equations for the EDGETRAN code are provided by a two-dimensional Monte Carlo recycling neutral transport code, NTRAN, in which the two major mechanisms by the recycling neutrals, i.e., electron impact ionization and charge exchange, are taken into account. The two major high-recycling characteristics of the parallel temperature gradient and the plasma pressure conservation are identified in this operation space along the magnetic flux tubes between the upstream position and the divertor target plate in the KSTAR tokamak. In addition, plasma temperatures T_t and densities n_t at the target plate and upstream temperatures T_u are scaled with the upstream plasma density n_u, and these scaling results are compared with those in a simple one-dimensional analytic plasma transport model, the so-called two-point model. Finally, the simulation shows that the peaked feature of the upstream ion temperature profile adjacent to the separatrix affects the distribution of the divertor heat flux. This implies that the ion parallel heat conduction near the separatrix plays an important role in determining the radial profile of the heat flux onto the divertor target as the electron parallel heat conduction does in this conduction-limited regime. It is therefore, suggested that modifying the upstream plasma property profiles makes it possible to control the power distribution at the divertor plate.

1. Introduction

The edge region of a tokamak is of great importance in both plasma confinement in the core region and divertor material protection from the hot core plasma, and a number of research activities on this region have been intensively conducted. The importance arises from the fact that most of the critical mechanisms of heat and particle transports are taking place in this region and, in turn, the successful

steady-state operation and device maintenance depend on how the divertor can effectively disperse plasma power exhausted from the main plasma, control impurity particles and remove the fuel and fusion by-products (usually He `ash'). Therefore, understanding of divertor physics is one of the most crucial tasks in tokamak research along with the issues of plasma confinement.

In particular, when the relations between global parameters (such as line-averaged density, auxiliary heating power or confinement time) and edge parameters (like separatrix density, upstream and divertor temperatures or divertor heat flux) are a matter of concern, it is important to investigate the plasma characteristics in the operation regimes with various divertor conditions depending on those global parameters[1]. Defining these divertor regimes with different plasma conditions also provides information on appropriate edge-related operational boundaries, i.e., operation windows regarding the extent of power deposition on the divertor and the approach to radiation instabilities such as the Multifaceted Asymmetric Radiation From the Edge (MARFE).

The divertor operation regimes are classified in order of increasing Coulomb collisionality[2] by raising the density at a constant input power in experiments. Another way to scan these operation regimes is to increase radiation losses at a constant upstream density so that the target temperature could lower. The divertor operations are usually classified into the two major regimes in accordance with the location of the major volumetric ionization source; *the attached regime* where the temperature at the target plate is high enough for the ionization front to stay 'attached' to the target, and *the detached regime* where the plate temperature falls to a few electron volts so that the ionization front moves towards the upstream and remains 'detached' from the plate[3]. In the attached regime, the divertor temperature is sufficiently high that friction processes could be neglected in comparison to ionization, while the plasma pressure is kept constant along the field line. The attached regime again is divided into the two subregimes based on an ability of the SOL to sustain a significant temperature difference between the upstream and the target; *linear (sheath-limited) regime* and *high-recycling (conduction-limited) regime*.

Although the detached plasma condition seems to be attractive in terms of divertor heat load and power reduction, high-recycling divertor operations are often considered beneficial to many experiments for some practical reasons[2]. First, it is always preferred to the sheath-limited regime not only due to the high upstream plasma temperature adjacent to the confined plasma in favor of the achievement of good core confinement but also due to the low divertor temperature reducing the physical sputtering from the plate. Although the detached condition has its advantage in the reduction of divertor heat load, the strong detachment often leads to the MARFE which, in turn, causes the tokamak to reach its density limit and to an eventual disruption[4]. The counterbalancing effect against this radiation instability is the thermal conduction capable of redistributing the heat to local radiation spots, which is most apparent in the conduction-limited regime.

According to a simple model that predicts peak heat loads and scales them with the heating power for the KSTAR tokamak designed to have the total input power of 15.5 MW in the baseline operation, the heating power should be lower than 14 MW in order not to exceed an engineering limit of 3.5 MW/m^2 for the divertor plate[5]. This indicates that the standard full power operation is not

achievable with a concept of high-recycling divertor due to the limitation to the heat load on the plates. Other operation modes like radiative divertor or radiating mantle operations are taken into account for reducing the heat load by lowering the temperature in the vicinity of the divertor plate.

However, the heating power at the initial stage of the KSTAR operation is not that high, and thus the study on the operation with lower heating power should not be ignored. Moreover, this low-power operation will cover some of the baseline operation modes. Hence, it is suggested that this aspect of divertor research is worth investigating by numerical simulations. Table 1 summarizes the values of heating power and pulse length for baseline operation phases in the KSTAR program which is being progressed for constructing a superconducting tokamak at the KBSI (Korea Basic Science Institute)[6].

Table 1. Heating powers planned for operation phases in the KSTAR program

Operation phases	(1) First plasma	(2) Ohmic plasma		(3) Baseline operation		
Pulse length (sec)	≥ 0.1	10 ≥	10 ≥	20 ≥	20 ≥	20 ≥
NBI (MW)	-	-	-	8	8	8
ICRH (MW)	-	-	-	-	6	6
LHCD (MW)	-	-	-	-	-	1.5
ECH (MW)	(0.5)	(0.5)	0	(0.5)	(0.5)	(0.5)
Total auxiliary heating (MW)	0.5 (Start-up)	0.5 (Start-up)	0	8.0 (0.5)	14.0 (0.5)	15.5 (0.5)

In this work, numerical calculations for the KSTAR tokamak are performed to find the operation space for a high-recycling divertor regime in terms of the upstream density and the input power and to investigate various edge plasma characteristics in this divertor operation regime. In the following, a numerical modeling of transport phenomena of plasma and neutrals in the edge region is summarized for the description of the EDGETRAN[7] and NTRAN[8] codes, respectively. Next, the simulation results calculated by the two codes are discussed by making suitable comparisons with an analytic model and other experimental evidences. The high-recycling characteristics of temperature difference and pressure balance between the upstream and the divertor are identified, and the scalings of divertor plasma parameters and the relationship between upstream conditions and divertor power dispersal are discussed. Finally, a summary of this work is presented.

2. Numerical Modeling

In order to calculate the plasma parameters such as ion and electron temperatures and densities in the SOL including the upstream position and the divertor region, the numerical simulations in this work use a two-dimensional two-fluid edge plasma transport code, EDGETRAN[7], developed at the Seoul National University. The source terms of particle, momentum and energy, which appear in the

plasma transport equations in the EDGETRAN code, are provided by calculations using a two-dimensional Monte-Carlo neutral transport code, NTRAN[8], also developed at the Seoul National University.

2.1. Two-dimensional Edge Plasma Transport

The moment equations formulated by Braginskii[9] are used to model the plasma transport phenomena in the edge region and these transport equations are appropriately modified by the assumption of quasineutrality ($n \equiv n_e \equiv n_i$) and negligible electron mass ($m_e << m_i$) in a two-fluid plasma. For equations of continuity,

$$\frac{\partial n}{\partial t} + \nabla\cdot(n\boldsymbol{u_i}) = S_n, \tag{1}$$

$$\nabla\cdot\boldsymbol{J} = 0. \tag{2}$$

For the electron and ion momentum balance equations, respectively,

$$-\nabla p_e + n\left[\nabla f - \left(\boldsymbol{u_i} - \frac{\boldsymbol{J}}{ne}\right)\times \boldsymbol{B}\right] + \boldsymbol{R_{ei}} = 0, \tag{3}$$

$$mn\left[\frac{\partial \boldsymbol{u_i}}{\partial t} + (\boldsymbol{u_i}\cdot\nabla)\boldsymbol{u_i}\right] = -\nabla p_i - \nabla\cdot\prod_i + \boldsymbol{J}\times\boldsymbol{B} + \boldsymbol{S_p} - m\boldsymbol{u_i}S_n. \tag{4}$$

For the electron and ion energy transport equations, respectively,

$$\begin{aligned}&\frac{3}{2}n\frac{\partial T_e}{\partial t} + T_e\nabla\cdot\left(n\boldsymbol{u_i} - \frac{\boldsymbol{J}}{e}\right) + \frac{5}{2}\left(n\boldsymbol{u_i} - \frac{\boldsymbol{J}}{e}\right)\cdot\nabla T_e + \nabla\cdot\boldsymbol{q_e} \\ &= -\boldsymbol{J}\cdot\nabla f + \boldsymbol{u_i}\cdot(\nabla p_e - \boldsymbol{J}\times\boldsymbol{B}) - Q_{ie} + W_e - \frac{3}{2}T_e S_n,\end{aligned} \tag{5}$$

$$\begin{aligned}&\frac{3}{2}n\frac{\partial T_i}{\partial t} + T_i\nabla\cdot(n\boldsymbol{u_i}) + \frac{5}{2}n\boldsymbol{u_i}\cdot\nabla T_i + \prod_i : \nabla\boldsymbol{u_i} + \nabla\cdot\boldsymbol{q_i} \\ &= \boldsymbol{u_i}\cdot(\nabla p_i - \boldsymbol{S_p}) + \left(\frac{1}{2}mu_i^2 - \frac{3}{2}T_i\right)S_n + Q_{ie} + W_i,\end{aligned} \tag{6}$$

where n is the plasma density, $\boldsymbol{u_i}$ the ion velocity, $\boldsymbol{J}$ the plasma current and f the electrostatic potential. The ion source term S_n by the ionization of neutral hydrogen and the momentum transfer vector $\boldsymbol{S_p}$ by recycling neutrals are added to the continuity equation (1) and the ion momentum equation (4), respectively. In addition to Q_{ie}, which represents the energy exchange between ions and electrons through collisions, W_e and W_i appear in the electron and ion energy balance equations, respectively. Here, W_e is the electron energy loss by the ionization of recycling neutrals and W_i stands for the ion energy change by charge exchange with neutrals and the ion energy gain by the ionization of recycling neutrals. These source terms, S_n, $\boldsymbol{S_p}$, W_e and W_i, are obtainable from calculations of neutral transport. Other implicit terms such as the mean momentum change $\boldsymbol{R_{ei}}$ of electrons due to collisions with ions, the shear stress P_i for ions, the heat flux densities $\boldsymbol{q_e}$ and $\boldsymbol{q_i}$, carried by electrons and ions, respectively, have their own expressions containing the main plasma variables n, $\boldsymbol{u_i}$ and T, and their derivatives. Their explicit expressions with various transport coefficients are mostly listed in Ref.[10] except for

the coefficients along the radial (cross-field) direction which are assumed to be anomalous in this code. The governing equations (1) to (6) are expanded in an orthogonal coordinate system based on the magnetic flux functions with a toroidal symmetry. The equi-flux lines are adopted as a coordinate in the radial direction (y) and the other coordinate in the poloidal direction (c) is created by making it orthogonally intersect the first coordinate.

Figure 1 depicts a calculated domain in the edge region of the KSTAR tokamak, and this domain is schematically simplified in Figure 2 to give the description of boundary conditions. The net parallel velocity and the derivatives of plasma density and temperature vanish on the symmetry planes, AB and CD. Heat fluxes to the plate are given at the divertor plate EF. On the private flux plate DE and the first wall FA, floating values of n, T_e and T_i are first guessed and then successively corrected during the iterations instead of giving fixed values. Boundary conditions on the separatrix line BC have been modified to accommodate reasonable physical circumstances including the properties of the core plasma, and the more detailed explanation about them is given in Ref.[11].

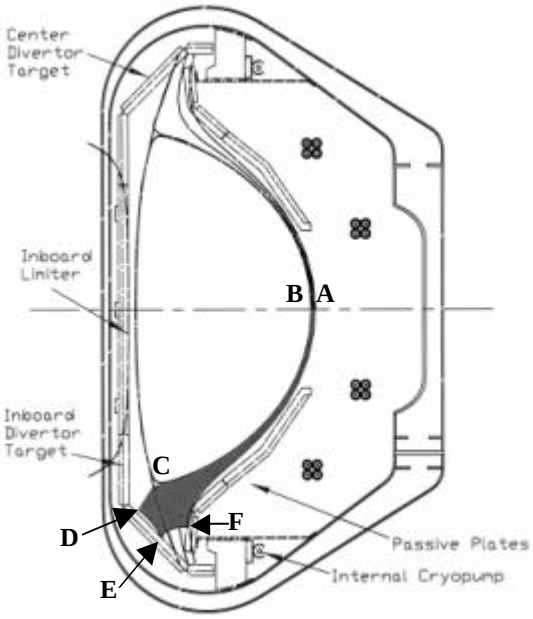

Figure 1. Calculated domain (shaded area) in the edge region of the KSTAR tokamak

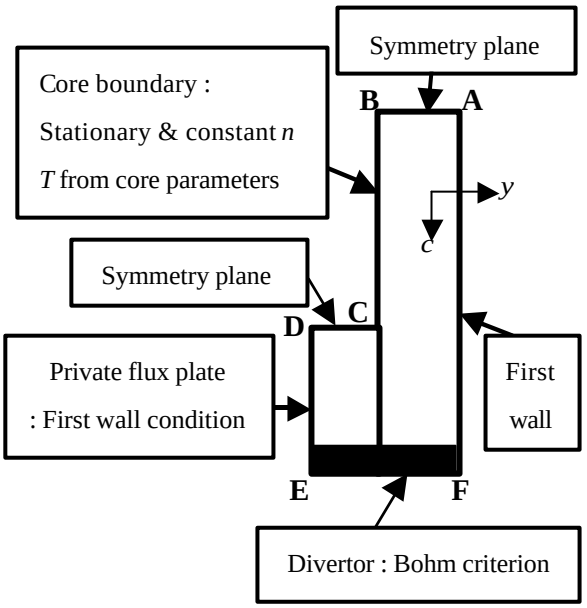

Figure 2. A schematically simplified geometry of the tokamak edge region with its boundary conditions described

2.2. Two-dimensional Recycling Neutral Transport

As mentioned in the preceding section, the source terms in the plasma transport equations for the EDGETRAN code should be calculated through the analyses of the recycling neutral transport phenomena. The recycling hydrogenic atoms and molecules are produced through the neutralization and reflection of incident ions on the divertor plate. They are backscattered and released into the edge plasma from the plate, giving rise to a number of atomic and molecular interactions with

background plasma ions and electrons. The molecules are usually dissociated into the atoms shortly after they are released, and the neutral atoms undergo either charge exchange process with plasma ions or ionization process by plasma electrons until they strike the wall or the separatrix. The two major atomic interactions of charge exchange with ions and electron impact ionization are included in the calculation, respectively,

$$D^0 + D^+ \rightarrow D^+ + D^0,$$
$$D^0 + e \rightarrow D^+ + 2e.$$

Other atomic interactions such as the neutral-neutral and neutral-ion elastic scattering processes are not considered due to their negligible contribution. In the charge exchange process, ions gain momentum and energy as considered in the terms $\boldsymbol{S_p}$ in Eq.(4) and W_i in Eq.(6), respectively. The particle source term S_n in Eq.(1) and the electron energy gain W_e in Eq(5) are obtained from the electron impact ionization process.

The NTRAN code is constructed based on the Monte Carlo numerical scheme in a two-dimensional geometry. To determine the kind of the atomic process, the neutral density and energy on each grid in the calculation domain, the background plasma density and energy on the grid point should be provided and this information is obtained from the EDGETRAN code. The ion influx to the target is also given by the EDGETRAN code to determine the number of incident ions to become neutrals. Therefore, the edge plasma fluid code and the Monte Carlo neutral particle code exchange their information on inputs and outputs by turns until a certain convergence criterion meets.

3. Calculation Results and Discussions

3.1. Operation Space for a High-recycling Divertor Regime

The EDGETRAN code has assumed non-ambipolar plasma motions so that it could describe the presence of self-consistent plasma currents. It is capable of calculating the radial and diamagnetic components of plasma flow velocity, electric current vector, electrostatic potential and electric fields, in addition to the main plasma properties such as plasma density, temperature and parallel flow velocity. In the present numerical work, however, only the main plasma properties are presented since they are of interest in analyzing the divertor operation regimes and in comparing their calculated values with those of an analytic model. Table 2 is a list of some device parameters of the KSTAR tokamak that are used as the input values for numerical simulations. In the EDGETRAN code, the particle and energy transports in the radial direction across the magnetic flux surfaces are assumed to be anomalous. Diffusion coefficient D and thermal diffusivities c_i and c_e are given in Table 2 for the KSTAR tokamak from the previous numerical calculations by the UEDGE code[5].

Since the high-recycling divertor operation regime is a matter of primary concern in the present numerical work, the edge plasma densities are scanned with various constant input heating powers to find this regime, and some operating windows appeared in the high-recycling regime are listed in Table 3 in terms of the input power supplied by auxiliary heating and the edge (pedestal) plasma

density. Some apparent evidences showing these density-power windows in the high-recycling divertor regime will be presented in the next two sections.

Table 2. Device parameters of the KSTAR tokamak used as the input values in the calculation

Parameters	Values
Major radius (R_0)	1.8 m
Minor radius (a)	0.5 m
Elongation (k)	2.0
Triangularity (d)	0.8
Toroidal magnetic field (B_T)	3.5 T
Plasma current (I_p)	2.0 MA
Number of null	2
Energy confinement time (t_e)	140 msec
Diffusion coefficient (D)	0.5 m^2/s
Thermal diffusivity for ions (c_i)	1.0 m^2/s
Thermal diffusivity for electrons (c_e)	1.0 m^2/s

Table 3. Operating windows of heating power and edge plasma density appeared in the high-recycling divertor regime

Auxiliary heating (MW)	Edge density ($10^{19} m^{-3}$)
4.5	2.1 ~ 2.5
5.0	2.9 ~ 3.3
5.5	3.7 ~ 4.1
6.0	4.4 ~ 4.9
6.5	5.1 ~ 5.7

3.2. High-recycling Characteristics

Among the plasma characteristics regarded as the evidences showing that an SOL plasma is in the high-recycling regime predicted in Table 3, two major features are discussed; the plasma temperature gradient and the pressure conservation along the flux tubes in the SOL ranging from the upstream symmetry plane to the divertor plate.

Parallel Plasma Temperature Gradient

Figure 3 describes the radial temperature profiles for ion and electron at the upstream position and the divertor plate. The values at the upstream position correspond to those obtained at the outer midplane. As seen in this figure, an apparent temperature difference between the two locations is observed regardless of species, and T_u is approximately $2T_t$ for the entire radial positions, revealing the conduction-limited feature in this regime. Also, the peaked profile of ion upstream temperature near

the separatrix line is sharper than that of electron one. This feature has been reported from a number of experiments[2][4][12], in which the ion temperatures were usually measured larger than $2T_e$ at the upstream. Although the upstream ion temperatures are much higher than electron ones near the separatrix, they become thermally equilibrated in the outer region apart from the separatrix as seen in this. This is regarded as an evidence of the strong parallel conduction to the divertor in the near separatrix area.

In the divertor target region, ion temperatures are higher than electron ones, which implies that the ion energy loss by charge exchange with neutrals is relatively weak compared to the electron energy loss by ionization. In other words, the high-recycling feature represents the overwhelming ionization process rather than charge exchange process. The temperatures in the target area are considerably higher than 5 eV, at which the charge exchange process begins to be significant. Such high temperature at the target plate in the simulation may be resulted from the negligence of radiative cooling mechanism either by neutral hydrogens or by impurities.

The relative importance of ionization process near the target can be inferred from Figure 4 where the temperature profiles of ion and electron along the separatrix line are plotted from X-point to target plate. While the ion temperature steadily decreases along the separatrix line, the gradient of electron temperature becomes steeper near the divertor, which implies the electron energy loss by ionization is significant near the divertor target. For there are no energy sources and sinks along the field line from the upstream to the X-point, no temperature changes along the parallel direction are expected in the upstream region above the X-point.

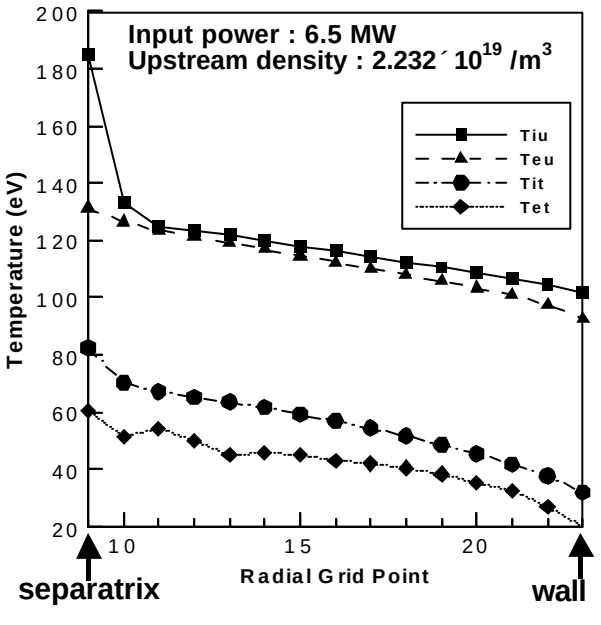

Figure 3. Radial profiles of ion and electron temperatures at the upstream and the divertor plate. The upstream density here corresponds to the edge (pedestal) density of $5.1 \times 10^{19}\,\mathrm{m}^{-3}$

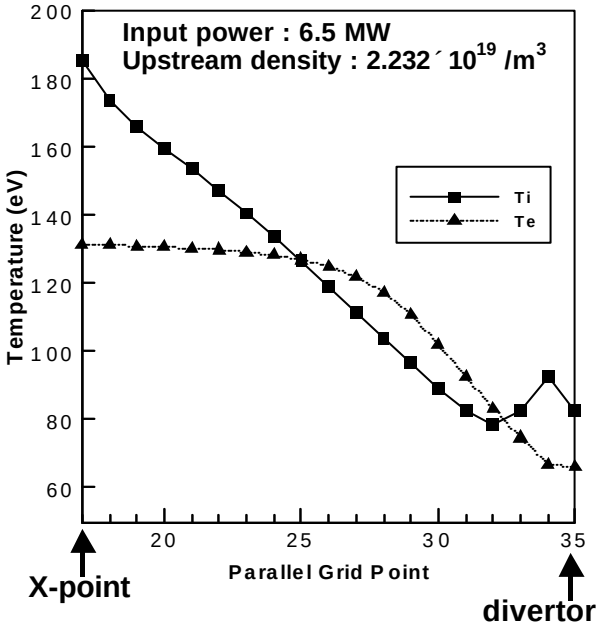

Figure 4. Parallel profiles of ion and electron temperatures along the separatrix line from X-point to divertor plate. The upstream density here corresponds to the edge (pedestal) density of $5.1 \times 10^{19}\,\mathrm{m}^{-3}$

Pressure Conservation

Ion pressures are also taken into account in this numerical simulation as well as electron pressures to evaluate the total plasma pressures at the upstream and the divertor plate. Figure 5 shows the total pressure values at the two regions, and the conservation of plasma pressure along the flux tubes over almost entire radial locations. Figure 6 shows the ratios of pressure values at the target to those at the upstream. These ratios are almost unchanged near a unity at any operating windows of edge plasma density for different heating powers given in Table 3. This suggests that the operating windows of edge density and input power given in Table 3 are in the high-recycling regime. The upstream density in Figure 6 corresponds to the edge (pedestal) density in Table 3.

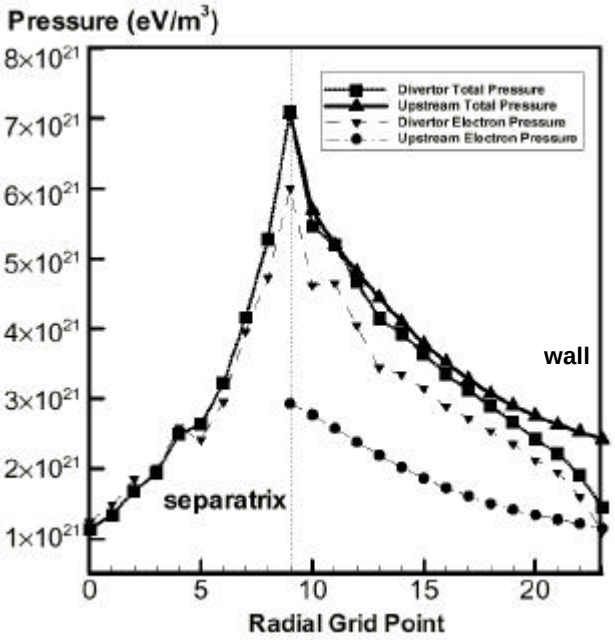

Figure 5. Radial profiles of the total (ion + electron) and electron pressures at the upstream and the divertor plate (input power : 6.5 MW, edge density : 5.1×10^{19} m^{-3})

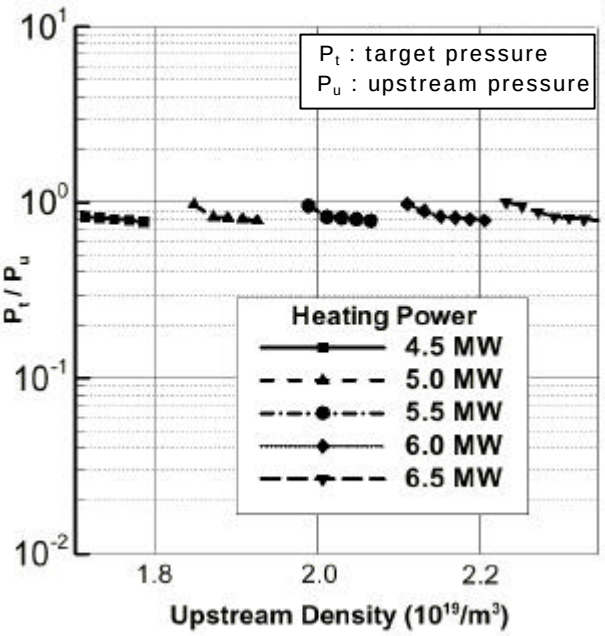

Figure 6. The ratios of target pressure to upstream pressure at the operating windows of upstream edge density for different input heating powers

3.3. Scaling of Upstream and Divertor Plasmas

Some of plasma properties at the target and the upstream are scaled with an externally specified parameter, i.e., upstream plasma density, and then the resulted scaling profiles are compared with the scalings obtained by a simple one-dimensional analytic plasma transport model, i.e., the so-called two-point model[4][13].

According to the two-point model in the high-recycling regime, upstream temperature T_u is

independent of upstream density n_u as far as input power is constant. However, it is practically expected that T_u with constant input power and no radiation process decreases as n_u increases. For a constant input power of 6.5 MW, the upstream density scanning has been done as presented in Figure 7(a) to see the variation of upstream temperature. The linear decrease of electron and ion upstream temperatures is observed as the upstream density increases.

The two-point model predicts the divertor temperature T_t varies as

$$T_t \propto \frac{1}{n_u^2}. \tag{7}$$

Again, the upstream density scanning for constant input power is plotted in Figure 7(b), which shows that the above relation (7) is valid for ions. In the case of electrons, the n_u^{-2}-dependence is rather weak and the decrease of electron temperature stops at a certain upstream density. This weak dependence of electron temperature at the divertor can be explained by the energy loss mechanism of each species. As the upstream density increases, the particle flux to the divertor plate also increases and this, in turn, increases the number of recycling neutrals. By the interactions of these recycling neutrals with plasma particles, the energies of electron and ion are exhausted and their temperatures decrease. A small amount of decrease in the plasma temperature makes a rather large difference between the rate coefficients of charge exchange and ionization, the latter being far more rapidly decreased. As the upstream density increases further, this difference gets more apparent and electrons lose less energy than ions do because of fewer and fewer ionization interactions by electrons. The existence of the plateau in the electron temperature profile at the target indicates the minimum divertor temperature that the plasma can reach in this operating regime. According to this relation in the high-recycling divertor regime, the goal of achieving a low plasma temperature near the divertor plate to reduce heat flux and physical sputtering is attainable simply by increasing the (upstream) plasma density.

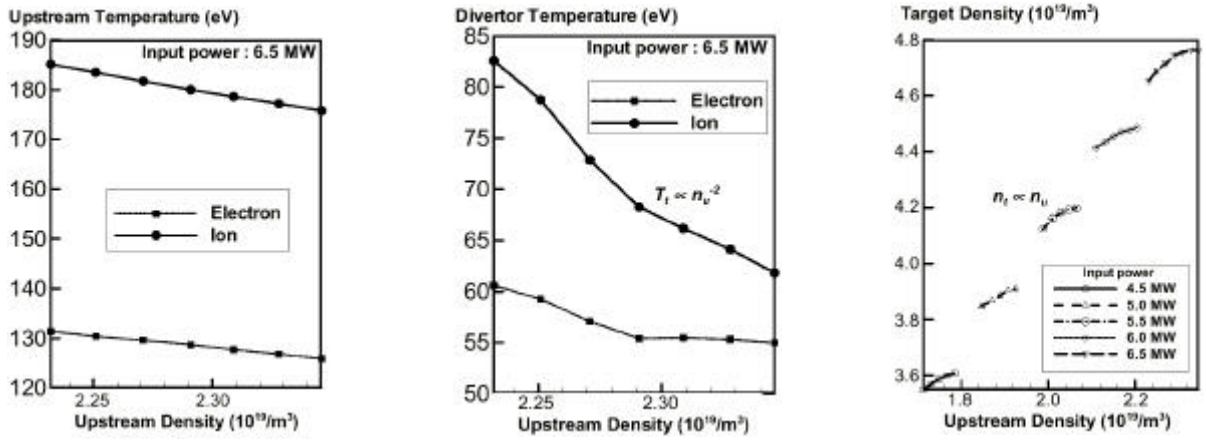

(a) (b) (c)

Figure 7. Scaling of (a) upstream temperature T_u, (b) divertor temperature T_t, and (c) divertor density n_t with upstream density n_u scanning for a constant input power of 6.5 MW.

In Figure 7(c), the result of density scanning is shown to find the relation between upstream density

n_u and target density n_t. The high-recycling feature of $n_t \mu n_u^3$, which is predicted in the two-point model, is not observed in the present result. The relation between n_t and n_u seen in Figure 7(c) bears a linear characteristic of $n_t \mu n_u$ as derived in the linear divertor operation regime. Therefore, the plasma conditions in these operating windows are considered to be not in the complete high-recycling regime but in a transition from the linear to high-recycling operation regimes[14].

3.4. Upstream Conditions and Divertor Power Dispersal

Figure 8 shows the profiles of total, kinetic and potential heat fluxes along the field line onto the divertor in the high-recycling regime with the increase of upstream density at a constant power of 6.5 MW. The total heat fluxes q_t have been calculated by an equation

$$q_t = n_t c_{St} (g_i T_{it} + g_e T_{et}) + n_t c_{St} e_{pot}, \tag{8}$$

where γ_i and γ_e are the sheath energy transmission coefficients for ion and electron and taken to be 3.0 and 5.5, respectively. The previous work in Ref.[7] did not include the potential heat flux, the second term in Eq.(8). Numerical computation in the present work, however, shows in Figure 8 that the contribution of potential heat fluxes are very small in this high-recycling divertor with high temperatures. A small drop in the heat flux with the increase of upstream density is also observed in this figure. In evaluating actual parallel heat fluxes to the divertor, a correction of a factor of ~ 0.7 is taken into account caused by the tilted angle of 45° between the divertor plate and the field line.

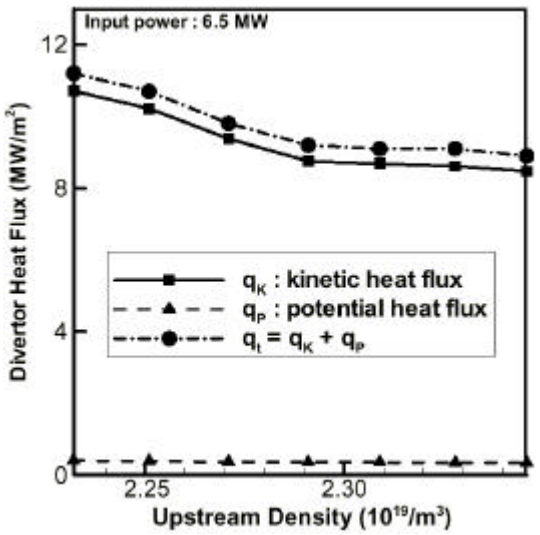

Figure 8. Dependencies of total, kinetic and potential heat fluxes parallel to the field line on upstream density of an input power of 6.5 MW

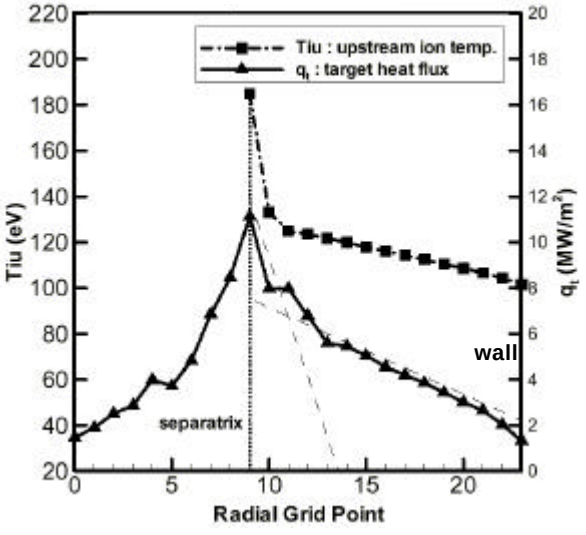

Figure 9. Comparison between radial profiles of upstream ion temperature and divertor heat flux (input power : 6.5 MW, upstream density : 2.232×10^{19} /m^3

Finally, an evidence of the correlation between the upstream plasma conditions and the target power dispersal is seen in Figure 9 for the radial profiles of upstream ion temperature and divertor heat flux.

The peaked feature near the separatrix appeared in the target heat flux profile resembles that in the upstream temperature profile. A power deposition gap on the plate very close to the separatrix line is nearly coincident with a narrow ion conduction channel determined by the upstream ion temperature profile besides the usual contribution of electron heat conduction[4]. Also, in this figure, the two power decay lengths exist in the target heat flux profile. This result mildly suggests that there is possibility to control the power distribution on the divertor plate by modifying the upstream plasma property profiles. However, one should be careful not to be misled by this result. It is the upstream profiles, not the absolute values themselves, what the heat profiles on the divertor are affected by. Therefore, merely increasing the upstream density does not guarantee a full solution to the power dispersal on the divertor plate even though it helps to lower the temperatures in this region.

4. Conclusions

The high-recycling characteristics in the upstream and divertor regions of the KSTAR tokamak have been observed by two-dimensional edge plasma and recycling neutral transport simulations. For numerical simulations, the EDGETRAN code for edge plasma transport and the NTRAN code for recycling neutral transport have been used.

A number of runs have been conducted in computing procedures to find the operating windows in terms of the edge (pedestal) density corresponding to the upstream density and the input heating power representing the high-recycling divertor regime. Although the input power ranges are rather lower than expected in the KSTAR standard operation modes, the operations with lower auxiliary heating power can not be ignored because they take a substantial portion in the initial stage of baseline operation phases in the KSTAR program as shown in Table 1.

The high-recycling divertor operation regimes have been featured by both the parallel gradient of plasma temperature and plasma pressure conservation along the flux tubes. The temperature difference obtained in this numerical simulation agrees well with those in the theoretical predictions by other authors[2][4][12], though they are not so remarkable as in the actual tokamak devices which shows $T_u \sim 10T_t$ in the high-recycling regime[14]. The peaked profiles adjacent to the separatrix in the upstream ion temperature and the divertor heat flux indicate that, not only the electron conduction but also the narrow ion conduction channel affects the divertor power distribution. Inclusion of ion pressure in calculating total plasma pressures at the upstream and the divertor plate has provided a firm evidence of pressure conservation in this regime. Radial temperature profiles for ion and electron at the divertor region in Figure 3 make certain that ionization process outweighs momentum transfer process by charge exchange.

The relationship between upstream plasma density and temperature is found as the linear decrease of temperature with the increase of density when radiative processes are not included. The density and temperature at the divertor could be scaled with upstream plasma density. In the case of divertor temperature, the scaling is similar to that of the two-point model prediction, while the divertor density

scaling has a linear feature ($n_t \mu n_u$) rather than a high-recycling one ($n_t \mu n_u^3$). This gives rise to the hypothesis that the regime under consideration is not in the complete high-recycling regime but the transition between linear and high-recycling regimes. The temperature scaling also reveals that the target temperature could reach its lowest value in this operation regime.

In addition, the similarity between the radial profiles of upstream temperature and divertor heat flux suggests possibility of controlling the divertor heat dispersal by manipulating the upstream plasma profiles but not the values themselves.

The high-recycling operations have their own advantages of retaining a hot plasma near the core and a pretty cold plasma near the divertor, and securing the density limit that the detached divertor operation can easily reach. Reactor-relevant tokamaks like ITER require the plasma temperature near the target plate to be much lower than that reachable in mid-size tokamaks with moderate input power. Both the temperature and the density near the divertor should be reduced so that a large input power, for example more than 100 MW for ITER, could be tolerated and effectively dispersed at the edge region by appropriate radiative cooling mechanisms such as radiative recombination significant in detached divertor operation regimes. For this reason, the study on detached regimes attracts attention as the future work taking the consideration of radiative process either by impurities or by hydrogenic atoms.

References

[1] S.J. Davies, S.K. Erents, P.C. Stangeby, J. Lingertat, G.F. Matthews, R.D. Monk and G.C. Vlases, J. Nucl. Mater., **266-269**, 1028 (1999)

[2] S.K. Erents, Nucl. Fusion **40**, 295 (2000)

[3] ITER Physics Expert Group on Divertor et al., Nucl. Fusion **39**, 2391 (1999)

[4] C.S. Pitcher and P.C. Stangeby, Plasma Phys. Control. Fusion **39**, 779 (1997)

[5] B.J. Lee, D. Hill, K.H. Im, L. Sevier, J.H. Han and B.J. Braams, Fusion Tech., **37**, 110 (2000)

[6] M.C. Kyum et al., T710-AT0-PM0-20000215/GSLee-E1-Iwd, Controlled Document, National Fusion R\&D Center, KBSI (2000)

[7] K.H. Im, Ph.D. Dissertation, Seoul National University, Seoul, Korea, 1995

[8] D.K. Kim, M.S. Thesis, Seoul National University, Seoul, Korea, 1995

[9] S. Braginskii, *Reviews of Plasma Physics*, Vol.1, p.205 (Consultants Bureau, N.Y., 1965)

[10] J.D. Huba, *1998 Revised NRL Plasma Formulary* (Naval Research Laboratory, Washington, DC, 1998)

[11] J.S. Ko, M.S. Thesis, Seoul National University, Seoul, Korea, 2001

[12] ITER Physics Basis Editors et al., Nucl. Fusion **39**, 2137 (1999)

[13] J.D. Galambos Y-K.M. Peng, J. Nucl. Mater., **121**, 205 (1984)

[14] C.S. Pitcher, Massachusetts Institute of Technology, private communication